2015

Targeting the Tight Junction Protein, Zonula Occludens-1, with the Connexin 43 Mimetic Peptide, Act-1 Reduces VEGF-Dependent RPE Pathophysiology

Elizabeth Christa Obert
Medical University of South Carolina

Targeting the tight junction protein, zonula occludens-1, with the connexin 43 mimetic peptide, αCT-1, reduces VEGF-dependent RPE pathophysiology by

Elisabeth Christa Obert

A dissertation submitted to the faculty of the Medical University of South Carolina in partial fulfillment of the requirements for the Master's Degree in the College of Graduate Studies.

Department of Neurosciences

2015

Approved by:

Bärbel Rohrer, Chairman of Advisory Committee

Committee Members:

Bärbel Rohrer

DeAnna Adkins

Carl Atkinson

Gautam Ghatnekar

List of Figures

List of Tables

Abstract

Age-related macular degeneration (AMD) is a multifactorial disease and is regarded as the predominant cause of central vision loss in the elderly in industrialized countries. A critical target tissue in AMD is the retinal pigment epithelium (RPE), which together with Bruch's membrane forms the outer blood-retina barrier (BRB). RPE-barrier dysfunction in AMD might result from attenuation and disruption of intercellular tight junctions. Zonula occludens-1 (ZO-1) is a major structural protein of intercellular junctions. A connexin-based peptide mimetic, αCT-1 (Alpha Connexin carboxy-Terminal 1), was developed which competitively inhibits ZO-1 interaction with its binding partners. We hypothesized that targeting ZO-1 signaling using αCT-1 would maintain BRB integrity and reduce RPE pathophysiology by stabilizing gap- and/or tight-junctions.

Choroidal neovascularization (CNV) was induced using laser-photocoagulation; RPE-cell barrier loss was triggered by bright light exposure (3000 lux for 3 hours). Both models lead to VEGF- dependent loss of cell junctions. The αCT-1 peptide was delivered via daily eyedrops. CNV lesion sizes were determined using optical coherence tomography (OCT). RPE flatmounts were stained for cell-junction proteins ZO-1 and occludin. Cell profiler software was used to examine the RPE tiling pattern. *In vitro* experiments using ARPE-19 cells showed that αCT-1 stabilizes intercellular tight junctions.

αCT1 treatment reduced CNV development and fluid leakage, and damage was correlated with disruption in cellular integrity of the surrounding RPE cells. Light-damage significantly disrupted RPE cell morphology, which was prevented by αCT-1 pre-treatment. *In vitro* experiments using ARPE-19 cell monolayers suggest that αCT-1 stabilizes intercellular tight junctions.

Taken together, stabilization of cellular junctions with αCT-1 was effective in ameliorating RPE dysfunction in AMD models of photo-coagulation-induced CNV and bright-light exposure RPE-cell barrier loss. Future research will include additional investigation into the peptide's mechanism of action.

Acknowledgements

First of all, I would like to express my special appreciation and gratitude to my major advisor, Professor Bärbel Rohrer, PhD for being a wonderful mentor throughout my research journey. Her motivation for scientific endeavor and knowledge were invaluable over the course of my master's thesis research. I also would like to especially thank her for her motivation and reassuring approach she shows towards her students.

I would like to express my special gratitude to my advisory committee, Professor Bärbel Rohrer, PhD; DeAnna Adkins, PhD; Carl Atkinson, PhD; Yiannis Koutalos, PhD; and Gautam Ghatnekar, PhD for their guidance in research and in scientific writing. I also would like to thank Christina Greg, PhD for critical review. The Rohrer Lab was paramount for a supportive experience from the very start of my graduate career and fond memories will be cherished. First String Research, Inc made this work possible.

Special thanks to my family for their support and optimism they exhibited throughout the three years of my master's research. My deepest appreciation goest to my mother, Patricia Obert, for her endless encouragement and patience throughout my schooling and my long-term career goals.

Chapter 1: Review of Literature

Overview of AMD

Age-related Macular Degeneration (AMD) is the most common cause of central visual impairment in the elderly. In the Unites States alone, 10% of individuals between 65 and 75 years of age have some degree of vision loss related to AMD.[1] The risk of getting AMD increases 15-fold in individuals over 75 years of age. With the population age only growing in industrialized countries, the prevalence of AMD will rise as well.[2] It is estimated that the prevalence of this disease will increase to around 3 million by 2020.[3]

AMD is a multifactorial disease of which the largest risk factor is aging. Other risk factors are of environmental as well as genetic nature. Polymorphisms in the complement control proteins factor H (CFH) and factor B (CFB), as well as complement receptor 2 (C2), are strongly associated with AMD.[4] In fact, approximately 50% of AMD cases have the risk allele (402H) while only 29% of the controls carry that particular variant in their genome.[5] The reason being is that a single mutation from tyrosine (Y) to histidine (H) at the 402 site of CFH is implicated in impaired regulation of the alternative pathway's complement activation.[4, 5] On the other hand, variants of CFB and C2 seem to be protective. Haplotype analysis revealed that possessing the protective allele L9H in BF and E318D inC2, as well as the variant intron 10 of C2 and the R32Q allele significantly reduces the risk of AMD.[6] It is important to note that there are synergistic effects of genetic and environmental agents that ultimately determine the risk factor of developing AMD. One environmental factor that is unequivocally linked to AMD is tobacco

smoking. It is thought that smoking increases the levels of oxidative stress, thereby, directly leading to damage to the retinal pigment epithelium (RPE) in AMD.[7]

AMD pathology involves the breakdown of the retinal pigment epithelium (RPE), a single layer of hexagonal, highly pigmented cells located between the retina and the choroid. The RPE displays a distinct apical and basal polarity with the photoreceptors being on the apical and the fenestrated choriocapillaris on the basal side. Hence, the RPE together with the BrM form part of the blood-retina barrier, ensuring the separation of the retina from the choroid circulation, and thus, maintaining the immune privilege of the eye.[8] Its many functions include: transport of molecules between the subretinal space and the choroidal blood supply; spatial ion buffering; secretion of growth factors that control the stability of photoreceptors, Bruch's Membrane (BrM) and the choroid; and modulation of the immune response.[8] Photoreceptor outer segment discs continuously renew themselves from the base due to the shedding of photo-generated oxidized outer-segment disc material.[9] The RPE is able to phagocytose photoreceptor outer segments via its microvilli on the apical aspect. Impaired function of the RPE to effectively remove and degrade this material can have deleterious effects on the retina's health.[8-10] The internalized discs that don't get properly degraded accumulate as lipofuscin granules in the lysosomal system. While lipofuscin granules naturally accrue with age, it is presumed that some of their contents, specifically A2E, are associated with RPE damage and AMD.[10, 11]

Two clinical forms of AMD exist: atrophic (dry) and exudative (wet). White or yellow fatty deposits (drusen) that build up between Bruch's membrane (BrM) and the retinal pigment epithelium (RPE) characterize the early stage of AMD. Normal aging contributes to small discrete hard drusen within the macula. However, the deposits that are linked to AMD are of soft nature and exceed 63 μM in diameter.[10, 12] In late AMD, in addition to drusen, patients exhibit damage to the macula, which can occur due to consequences of geographic atrophy (GA) or choroidal neovascularization (CNV). In GA, the advanced form of dry AMD, the RPE starts to atrophy, thereby leading to the degeneration of photoreceptors. Thus, vision is far more impaired in GA than in early dry AMD that bears little consequence to vision. Wet AMD on the other hand, is characterized by the growth of new blood vessels that break through the blood-retina barrier and grow into the retina under the macula. These blood vessels tend to be fragile and often leak blood and fluid. This phenomenon is termed CNV and is associated with rapid and severe vision loss. While only 10 – 15% of AMD cases develop into the exudative form of the disease, it accounts for more than 80% of the individuals who are legally blind due to AMD.[13]

RPE damage and loss of blood-retina barrier function is a common feature in dry and wet AMD, where the pro-angiogenic factor, vascular endothelial growth factor (VEGF), plays a critical role.[12] The RPE naturally secretes low concentrations of VEGF to the basal side of the RPE, where the growth factors are needed to stabilize the choroidal endothelium.[14] In response to an injury and damage, the RPE secretes high levels of VEGF on the apical and basal side, inducing RPE permeability and potentially harmful neovascularization in

the choroid.[15] Leaky blood vessels and RPE permeability are the result of VEGF altering tight junction function in the respective locations.[16]

The RPE exhibits three kinds of cell junctions: tight, adherens and gap junctions. Tight junctions form a gate or barrier that regulates the paracellular diffusion of solutes and nutrients in the RPE.[17] Adherens junctions provide the strong mechanical attachment between adjacent RPE cells that occurs prior to the formation of tight junctions.[18] Together with tight junctions, adherens junctions afford the barrier function of the RPE, while gap junctions allow for the communication between cells within the RPE monolayer.[19]

Overview of Cell Junctions

The apical junctional complex consists of two distinct cell junctions: tight and adherens junctions.[20] The tight junctions comprise of at least 40 proteins some of which are categorized into three transmembrane proteins: claudin, occludin and adhesion proteins that mediate intercellular adhesion such as junctional adhesion molecule (JAM).[21, 22] Other proteins are intracellular scaffold proteins that link the junctions to the cytoskeleton. Claudins make up the backbone of the tight junction complex, as they are able to polymerize, forming the tight junction strands necessary gating properties.[23] Currently, 24 members of the claudin family have been discovered. They are implicated in the regulation of tight junction ion selectivity, some of which result into the formation of cation or anion selective pores. Occludin is an important tight junction protein that plays more of a regulatory role of maintaining and organizing the tight junction structure,

but is neither necessary nor sufficient for its survival.[24] The main element in adherens junctions is the cadherin receptors that bridge the gap between neighboring cell membranes through homophilic interactions. In adherens junctions, catenins are the main scaffolding proteins that act to tether these junctions to the cytoskeleton.[25]

Gap junctions allow for a direct and rapid diffusion of second messengers, nutrients and metabolites that are smaller than around 1000 Daltons.[19] This form of communication plays a critical role in cellular regulations such as differentiation and proliferation, as well as protection and cell death via the bystander effect.[26] The basic unit of a gap junction channel is the connexin, a tetraspan transmembrane protein. Twenty-one connexin isoforms have been identified in the human genome, each with a distinct spatial and temporal expression pattern.[27] The RPE expresses Connexin43 (Cx43) and Connexin46 (Cx46).[28] Six connexins assemble into one connexon (hemichannel), while two connexons from adjacent cells join together to form a gap junction.[29] Various heteromeric configurations of different connexin proteins can occur during the assembly of a connexon, leading to different communication properties of gap junctions.[28]

Role of ZO-1

Zonula occludens-1 (ZO-1) is a scaffolding protein that binds to all three junction types, anchoring their respective cell junction molecules to the cytoplasmic actin. ZO-1 belongs to the family of membrane-associated guanylate kinase-like proteins (MAGUK) and carries three PDZ domains: an SH3 domain, a GUK domain and a proline-rich domain at the C-terminus.[30] The different domains afford interactions with junctional

transmembrane proteins (i.e., connexins) as well as their peripheral cytoplasmic scaffolding proteins. The binding of Cx43 to the PDZ2 domain of ZO-1 mediates the size and stability of gap junction channel aggregates.[31, 32] ZO-1 regulates the cellular distribution of Cx43, providing a control point for dynamic switching between gap junctional communication and non-junctional (hemichannel) communication.[32, 33] ZO-1 disruption in a functional epithelial monolayer results in a loss of barrier function as well as a reorganization of apical actin and myosin.[30, 34] Important for the context of AMD, VEGF disrupts ZO-1 organization, resulting in tight junction disassembly and increased monolayer permeability.[35, 36] VEGF-induced occludin phosphorylation of serine 490 resulted in decreased ZO-1 binding to occludin's C-terminus domain, concomitant with the defragmentation and ubiquitination of tight junctions. Furthermore, *in vitro* studies using endothelial cells show that VEGF-mediated disruption of gap junction communication is correlated with changes in Cx43 phosphorylation.[37]

Role of αCT-1

A synthetic peptide (25 amino acids with MW = 3597.33) was developed that contains a sequence mimicking the Cx43 C-terminal PDZ binding domain to target the interaction between Cx43 and its binding partners containing a PDZ2 binding motif.[31] The αCT-1 (Alpha Connexin carboxy-Terminal 1) peptide has a high binding-specificity with the PDZ-2 domain of ZO-1 and competitively inhibits ZO-1 interaction with its binding partners, such as claudins, occludin and Cx43.[31, 38, 39] Hunter has shown that inhibiting the ZO-1/Cx43 interaction increases the size of the gap junction plaque by increasing the proportion of hemichannels forming gap junctions with the adjacent cells compared to

undocked connexons in the plasma membrane.[31] Unpaired hemichannels allow for autocrine as well as paracrine intercellular communication, regulating the release of extracellular messengers such as ATP.[40, 41] Release of ATP can promote proinflammatory responses such as leukocyte chemotaxis, NO generation, cytokine release, or cytotoxicity.[40] Thus, stabilizing gap junction or tight junction function by preventing or reducing the interaction of ZO-1 with its binding partners via the αCT-1 peptide can be helpful in treating diseases where the cell junctions and their given functions are impaired.

Treatment with the peptide has been shown to have positive effects on treating cardiomyopathies[42-45] and on wound healing.[46-50] As gap junctional Cx43 is implicated in wound regeneration and scarring, the αCT-1 peptide was studied in models of cutaneous and corneal wound injury. Treatment with the peptide not only accelerated wound healing, but reduced the formation of scars in the tissue as well.[46, 48, 51] A similar effect is to be seen in the heart, where a myocardial infarction can lead to the disruption of gap junction organization, which in turn, can result into re-entrant arrhythmias and overall heart failure.[42, 43, 45] Application of αCT-1 to infarcted hearts reduced the propensity for arrhythmia as well as increased cardiac contractile function, improving the heart's mechanical function after injury. [42, 43, 45] Given that RPE cells are equally as dependent on healthy cell junction functions as are cardiovascular and skin tissues, we wanted to test the effects of the peptide on retinal diseases involving the RPE. Knowing that AMD is the result of decreased RPE/BrM barrier function, we propose that stabilizing the RPE cell junctions by treating with αCT1 will reduce AMD-like pathology.

Rationale And Aims

AMD is a multifactorial disease and is regarded as the most common of central vision loss in individuals over 65 years of age in Western countries. As a consequence of the exponential population aging, the projected number of people with AMD in 2020 is 196 million, increasing to 288 million in 2040.[52] The loss of visual acuity seen in individuals affected by AMD has a major impact on the quality of life as well as causing a significant economic burden to society.[2]

Two clinical forms of AMD exist: dry (atrophic) and wet (exudative). Dry AMD is characterized by a more progressive vision loss than in the wet form of the disease, where vision impairment is far more acute and severe.[13] While the atrophic form is far more prevalent, no FDA approved treatment options are currently available for dry AMD. Advancements in the management of the exudative form of AMD have been made, however, these treatments are expensive and not available to all patients in all countries.[52] Treatment options involve monthly or even bimonthly intraocular injections with anti-VEGF agents. As VEGF is the main pro-angiogenic factor involved in CNV, the hallmark of wet AMD, reducing the levels of VEGF in the retina and BrM can inhibit the progression of exudative AMD. However, not only is treatment via intravitreal injections very invasive, but it has also recently been published that patients receiving these injections can develop geographic atrophy, the late dry form of AMD. Hence, it is critical to further research the underlining mechanisms of AMD and the role that VEGF plays in wet as well as dry AMD in order to advance the treatment options for AMD.

The main target tissue affected by all types of AMD is the RPE. The RPE is a monolayer of cuboidal shaped cells that serves various factors important for visual function including secreting growth factors (including VEGF) and nutrients to the retina and choroid as well as the general stability of these layers. And finally, the RPE with the BrM acts as an important barrier, separating the choroidal vasculature from the neuronal retina. Tight junctions, regulating the flow of molecules between the apical and basal lateral compartments, thereby, controlling paracellular permeability and communication mediate this barrier. Gap junction channels, on the other hand, enable intercellular communication and the diffusion of ions and metabolites between connecting cells. Thus, preventing the breakdown of the RPE by stabilizing the different cell junctions involved in the various functions of the RPE offers therapeutic opportunity in the treatment of AMD.

Hypothesis

The αCT-1 peptide with its soluble design allows for intracellular translocation due to an antennapedia complex included to the peptide sequence.[48] There is substantial evidence that the peptide controls cell junction function in wound healing and cardiomyopathies, and therefore, reduces inflammation preventing a progression of the disease.[43, 45-47] We propose that the peptide will counteract the RPE/BrM breakdown by maintaining the barrier and communication function in the RPE and decreasing chronic inflammatory response (i.e. VEGF) along with oxidative stress associated with AMD. We tested this hypothesis in two different mouse models: the CNV model that mimics the angiogenesis seen in wet AMD, as well as the light damage model which shows loss of RPE cell

integrity akin to dry AMD. ARPE-19 cells were employed to determine the drug's mechanism of action.

Aim 1: Establish αCT-1 as a treatment paradigm in two VEGF-dependent *in vivo* models of AMD

Aim 2: Examine effects of the αCT-1 peptide *in vitro* on ARPE-19 cells to study the drug's mechanism of action

Chapter 2: Specific Aim 1

Establish αCT-1 as a treatment paradigm in two VEGF-dependent *in vivo* models of AMD

We tested the biological function of the Cx43 C-terminus mimetic αCT-1 peptide on two murine models of AMD. Mice do not develop AMD as they lack a macula, however, the structural anatomy and the primary site of AMD (RPE, BrM and choriocapillaris) are preserved from rodents to humans, making mice nevertheless attractive candidates for AMD research.[10] Hence, AMD-like pathology must be induced in mice to study the peptide's treatment efficacy via eye drop application (formulated in 0.05% Brij-78 and 0.9% NaCl) as well as its therapeutic window.

The Rohrer Lab has established a model of laser-induced CNV to examine the underlining mechanisms involved in wet AMD.[53] This model has confirmed the involvement of complement activation, oxidative stress, and more importantly for this study, elevated VEGF levels as contributing factors as well as providing evidence of efficacious treatment strategies targeting said factors.[53-55] Four CNV lesions with a spot size of 100 μm are generated via laser photocoagulation of the Bruch's membrane surrounding the optic nerve. These lesions increase radially over time and can be monitored via Optical Coherence Tomography (OCT), a diagnostic tool that allows for *in vivo* imaging of the retina and BrM. In addition, lesions and the surrounding area can be examined with cell junction markers, such as ZO-1 and occludin to study the morphology of cells. And finally, electroretinography (ERG) can be conducted on CNV'd animals to compare retinal function between αCT-1-treated animals and controls. It has been shown

that CNV lesions correlate in a drop in ERG amplitudes and the amount of vision loss correlates with the size of the CNV lesion.[5, 53, 54] The effects of the αCT-1 peptide will be examined on tight junction stabilization during CNV growth and on the retina function post photocoagulation.

Light-induced loss of the blood retina barrier is characterized by structural and functional similarities to pathologies in dry AMD. Cachafeiro has shown that hyperactivation of light leads to photoreceptor cell death that is mediated by VEGF and RPE permeability.[56] Albino mice are exposed to bright light under 3000 lux for 3 hours and RPE morphology was examined 24 hours after bright light exposure by immunohistochemistry between non light-damaged controls, light-damaged vehicle mice and light-damaged αCT1-treated animals. Morphometric analysis was conducted via the cell profiler software. In order to determine the treatment window for αCT-1 application, albino animals were divided in groups, administering only one dose of treatment at a time point either before or after bright-light exposure. The cell profiler software was used to determine the tiling pattern of the RPE and its morphology for each time point.

Materials and Methods

Animals

Albino Balb/c mice were generated from breeding pairs obtained from Harlan Laboratories. Pigmented C57BL/6J mice were based on Jackson Laboratory breeding colonies. The animals were housed in the Medical University of South Carolina animal care facility under a 12-hour light / 12-hour dark cycle with access to food and water *ad libitum*. All experiments were conducted in accordance with the ARVO Statement for the Use of Animals in Ophthalmic and Vision Research and were approved by the Institutional Animal Care and Use Committee.

αCT-1 Peptide Treatment

For *in vivo* studies, the αCT-1 peptide (FirstString Research, Inc., Mount Pleasant, SC) was administered via eye drops (5 mM; 10 μL per eye) formulated in a 0.05% Brij-78 and 0.9% NaCl solution. The control group received vehicle solution. The treatment schedule varied for individual experiments. Cell culture experiments were performed with 100 μM αCT-1, diluted in sterile water. A one-hour pre-incubation period of αCT-1 was employed for all *in vitro* experiments.

Laser-Induced CNV and Treatment Schedule

To induce CNV lesions, 3- to 4-month-old C57BL/6J mice were anesthetized (xylazine and ketamine, 20 and 80 mg/kg, respectively) as previously described.[53] Mouse pupils were dilated using 2.5% phenylephrine HCL and 1% atropine sulfate. In order to avoid cataract formation, mice were treated with Goniovisc (HUB Pharmaceuticals) before and

after lasering. Laser photocoagulation was induced via a 532 nm Argon laser (100 μM spot size, 0.1 s duration, 100 mW), in which 4 equidistant laser lesions were produced surrounding the optic nerve. The formation of a bubble at the site of photocoagulation indicated the desired rupture of the Bruch's membrane.[54]

Three αCT-1 peptide treatment regimens were employed for CNV studies in order to establish the treatment window of the drug. For the early administration model, mice were treated twice a day (am and pm) for the first three days post laser photocoagulation. In the continuous treatment paradigm, the animals were only given eye drops once a day throughout the 6-day experiment. Finally, the effects of the αCT-1 peptide were investigated when treating the animals twice daily (am and pm) during the last three days of the CNV study. Thus, all three treatment regimens resulted in equal drug exposure. Animals were euthanized on day 6 or 7 (depending on the experiment) in order to obtain RPE/choroid samples for immunofluorescence studies (see Immunofluorescence Staining).

Assessment of CNV Lesions

CNV size was determined using optical coherent tomography (OCT) on day 5 given that maximal CNV size was reported on that day.[57] OCT was performed using an SD-OCT system (Bioptigen Inc., Durham, NC), with scan parameters set to 1.6 x 1.6 mm rectangular volume scans, consisting of 100 B-scans (1000 A-scans per B scan). Mice were anesthetized and pupils were dilated as described above. Using the Bioptigen SD-OCT system, the center of the lesion was determined by identifying the midline of the

RPE/Bruch's membrane rupture,[57] and Image J software (http://imagej.nih.gov/ij/) was used to measure the cross-sectional area of the hyporeflective spot seen in the fundus image (en face) as well as the area of fluid accumulation in the outer retina (cross sectional view).

Electroretinography

Electroretinography (ERG) recordings were performed as previously described.[58, 59] In short, C57BL/6J mice were dark-adapted overnight and anesthetized with xylazine and ketamine (20 and 80 mg/kg, respectively). Pupils were dilated with phenylephrine HCL (2.5%) and atropine (1%). ERGs were recorded with the UTAS-2000 (LKC Technologies, Inc., Gaithersburg, MD) system, using a Grass strobe-flash stimulus. Stimuli consisted of 10 μs single flashes at a fixed intensity (2.48 cd*s/m^2) under scotopic conditions. ERG measurements were performed before (baseline ERG) laser photocoagulation and afterwards on day 6. A-wave amplitudes were measured from baseline to the a-wave trough, whereas b-wave amplitudes were measured from the a-wave trough to the peak of the b-wave.

Bright Light Exposure Protocol and Treatment Schedule

Six-week-old Balb/c mice were exposed to bright light for 3 hours using 3000 lux after 12 hours of dark adaptation.[60] The light exposure box was wrapped in aluminum foil to increase reflectivity. Mouse pupils were dilated using 2.5% phenylephrine HCL and 1% atropine sulfate 15 minutes prior to exposure of bright light.

Different treatment groups were established. To demonstrate proof of principle, animals received αCT-1 eye drops (5mM, see αCT-1 Peptide Treatment) three and one hours prior to the start of light damage, as well as 15 minutes after completion of light exposure. The control group was given vehicle drops at the same time points. For comparison, one group of animals did not receive any bright-light exposure. To establish the therapeutic window for αCT-1, 7 additional groups of mice were treated 4, 2, and 1 hour prior to bright-light exposure, as well as 1, 2, 4 and 6 hours post bright-light exposure. All animals were euthanized 24 hours post light damage in order to collect RPE/choroid flatmounts. RPE cells were stained (see Immunofluorescence Staining) with ZO-1 and occludin for morphometric analysis via the cell profiler software (cellprofiler.com).

Immunofluorescence Staining

Eyes were collected, and lens, anterior chamber and retinas were removed.[53] Eyecups were immersion-fixed in 4% paraformaldehyde (PFA) overnight at 4ºC. After extensive washing, eyecups were either incubated in antibodies recognizing ZO-1 (1:200; Invitrogen), occludin (1:200; Invitrogen) or connexin43 (1:300; Sigma Aldrich) in blocking solution (10% normal goat serum, and 0.4% Triton-X in tris-buffered saline). All before mentioned antibodies are rabbit polyclonal; thus, Alexa Fluor 488 goat-anti-rabbit (1:500; Invitrogen) was used as the secondary antibody. Following extensive washing, eyecups were flattened using four relaxing cuts and cover-slipped using Fluoromount (Southern Biotechnology Associates, Inc., Birmingham, AL). All immunohistochemistry experiments included a no-primary antibody control. Staining of

flatmounts was examined via fluorescence microscopy (Zeiss, Thornwood, NY) equipped with a digital black-and-white camera (Spot camera; Diagnostic Instruments, Sterling Heights, MI).

Assessment of RPE Morphology

Images of flatmounts (tiff) were imported into CellProfiler 2.1.1 for analysis (http://www.cellprofiler.org/). For each comparison, images of equal size and exposure time were analyzed, using a customizable script. The pipeline "neighboring cells" was used. For each image, we obtained cell count (number of cells present), form factor (equals 1 for a perfectly circular object), eccentricity (measures the degree to which an object represents an ellipse, and varies between 0 and 1), number of neighbors (a perfect hexagonal RPE cell has 6 neighbors), perimeter (the total length of the perimeter of all the RPE cells present in the image), and the total area covered by the RPE cells (determines the degree of loss of cells). Results were exported into Excel for statistical analysis.

Statistical Analysis

Data are presented as mean ± SEM. Single comparisons were analyzed by *t* test analysis, accepting a significance level of $P < 0.05$. Repeated ANOVA measurements were conducted for ERG studies.

Results

In order to test the biological function of the αCT-1 peptide, we needed to confirm that the drug does reach into the RPE via corneal eye drop application. The drug was further tested on two VEGF-induced *in vivo* models of AMD to establish it as a therapeutic option for this disease.

I. Detection of αCT-1 in RPE Cells

αCT1 peptide was applied via corneal eye drop application (5 mM) 4 hours prior to enucleation of the eyes. To confirm that αCT-1 reached its target via this route, we stained for Cx43 in murine flatmount preparations. Given that the αCT-1 is a peptide mimetic of the C-terminal sequence of Cx43, we could compare the difference in the Cx43 staining pattern between animals that were treated with αCT-1 when compared to vehicle. As expected, the vehicle control animals showed Cx43 staining mostly in clusters along the lateral walls of the RPE, representing Cx43 in gap junctions (**Fig. 1B**). In comparison, the flatmount from the animal that was given αCT-1 eye drops showed significantly more Cx43 staining both in gap junctions as well as in the cytoplasmic compartment (**Fig. 1C**). No staining was detected in no-primary antibody controls. These data confirmed that αCT1 applied to the cornea can reach the intended target tissue in quantities detectable by immunohistochemistry.

Figure 1

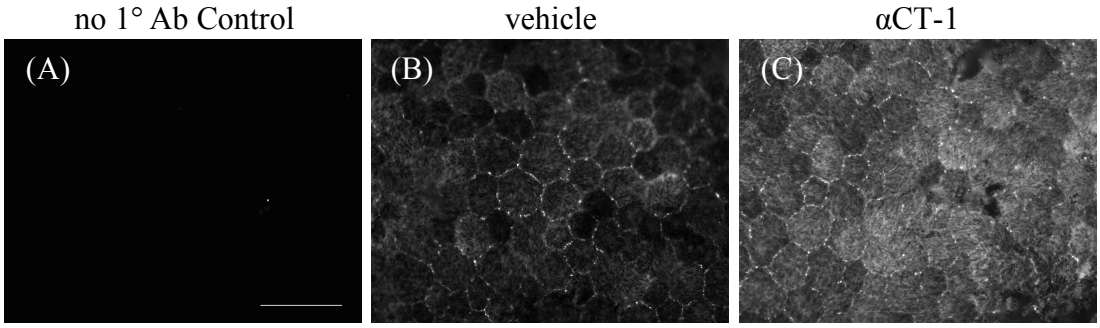

Figure 1. αCT1 detection in murine RPE flatmounts. The αCT-1 peptide has an amino acid sequence that is mimetic of the Cx43 C-terminal sequence. Thus, the peptide can be detected via Cx43 antibody that recognizes the C-terminal domain. The eyes of the mouse that received the peptide were enucleated 4 hours after eye drop administration and stained for Cx43. The αCT-1 peptide could be clearly detected in the animal that received the treatment drops (**C**), when compared to vehicle-treated animals **(B)**. No primary antibody was used as a control **(A)**.

II. Effects of αCT1 in a Model of CNV

II-A. αCT1 Peptide Decreases CNV Development

CNV is known to lead to an increase in angiogenic factor VEGF expression in both mouse and human RPE,[53] and CNV is associated with blood vessel growth and fluid leakage. In order to investigate the effects of the αCT-1 peptide on CNV development in 3- to 4-month-old C57BL/6J mice, CNV lesions were induced by laser photocoagulation of BrM. Area measurements of CNV lesion size (en face images) **(Fig. 3A, B)** and area of fluid leakage (vertical section) **(Fig. 3C, D)** were analyzed by SD-OCT. In **Figure 2**, we established the peptide's therapeutic dose to be 5mM, thus for further experiments, the peptide was administered via eye drops (5 mM of αCT-1; 10 μL per eye) and its efficacy was compared to vehicle drops in three different treatment regimes. All animals were exposed to equal drug treatment with the exception of timing in order to investigate the treatment window of the drug. Treatment was either provided continuously (mice were treated once [in the pm] on days 1-6 or 4-9) **(Fig. 4B, D)**; during the early phase of the model (animals were treated twice [in the am and pm] on days 1-3) **(Fig. 4A)**; or during the growth phase of the lesion (animals were treated twice [in the am and pm] on days 4-6) **(Fig. 4C)**. αCT-1 was found to significantly reduce the growth of the CNV lesion by around 25% ($P < 0.05$) in both the 6-day continuous **(Fig. 4B)**, as well as the 3-day early administration group (Fig. 3A). However, no significance could be established for the group that received treatment for 3-days late in the development of CNV **(Fig. 4C)** or those that received the delayed 6-day continuous treatment **(Fig. 4D)**. Importantly, αCT-1 was found to not only reduce the size of the fibrovascular scar **(Fig. 4, left-hand column)**, but also to significantly reduce the amount of fluid leakage into the subretinal

space **(Fig. 4, right-hand column)** by around 50% ($P < 0.05$) in both the early 6-day continuous, as well as the 3-day early administration group. As seen for growth assessments, no significance could be established regarding fluid leakage for the groups receiving αCT-1 treatment for 3 days in late CNV or those receiving the delayed 6 day treatment. These data together suggest that the αCT-1 peptide is required during the early phase of CNV to exert its effect on reducing both angiogenesis and fluid leakage.

Figure 2

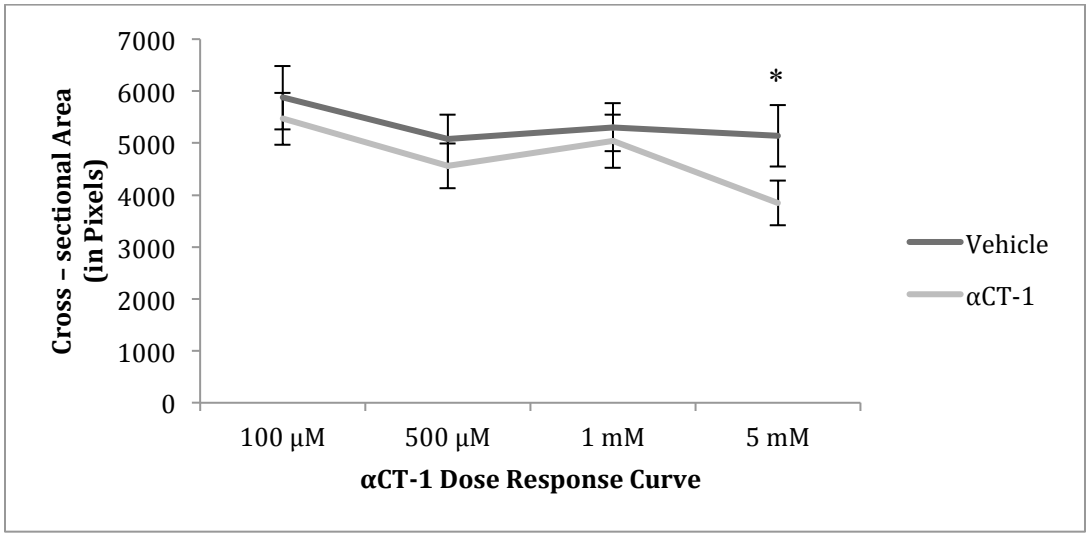

Figure 2. Dose efficacy of αCT-1 in *in vivo* models. The αCT-1 peptide was administered via eye drops (100 µM, 500 µM, 1 mM or 5 mM; formulated in 0.05% Brij-78 and 0.9% NaCl; 10 mL per eye) and its efficacy was compared to vehicle. An asterisk denotes significance (P <0.05) comparing vehicle group and αCT-1-treated animals. Data are expressed as mean ±SEM (n = 3-8 per treatment group).

Figure 3

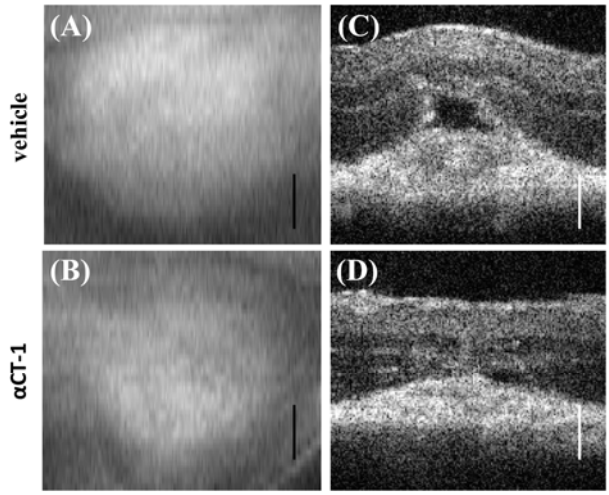

Figure 3. Imaging of choroidal neovascularization and fluid leakage in αCT-1- versus vehicle-treated mice. Animals were analyzed on day 5 post laser-photocoagulation by SD-OCT. The cross-sectional area of the hyporeflective spot seen in the fundus image **(A, B)** as well as the area of fluid accumulation in the outer retina **(C, D)** were determined and representative OCT images taken from the vehicle **(A, C)** and αCT-1-treated animals **(B, D)** are depicted.

Figure 4

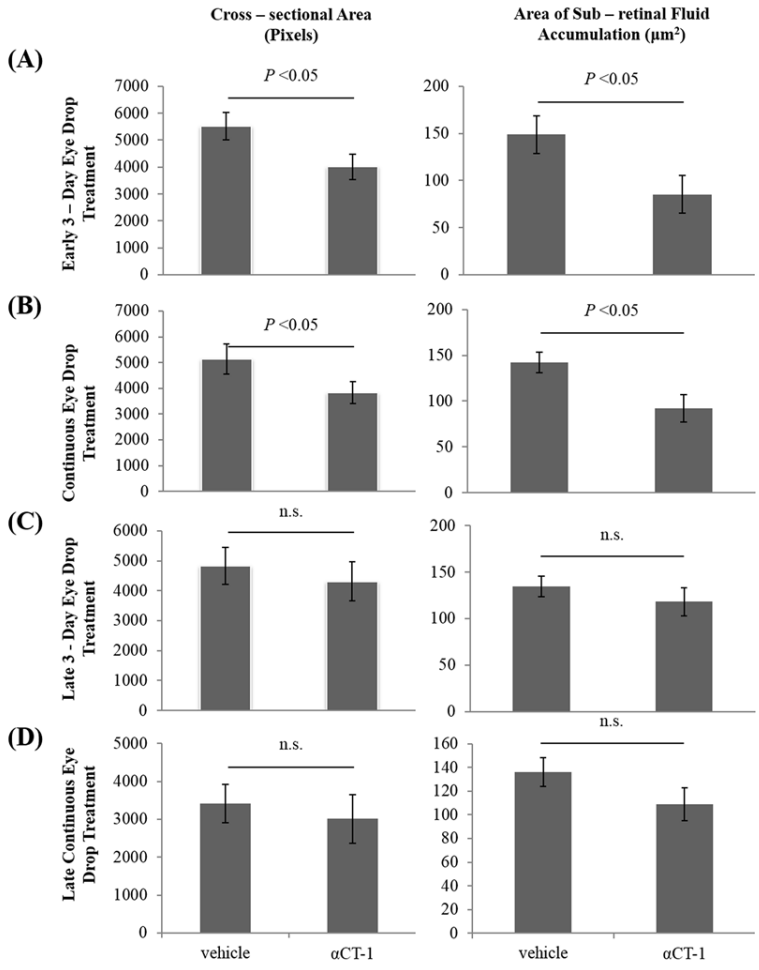

Figure 4. Analysis of cross-sectional area and fluid accumulation in αCT-1- versus vehicle- treated mice. CNV area and fluid accumulation were determined from SD-OCT images as depicted in Figure 2. Quantification of the cross-sectional areas of the lesions (left-hand column) as well as areas of fluid accumulation (right-hand column) were measured in pixels for the individual treatment groups. CNV size and area of fluid accumulation in αCT1-treated animals was reduced compared to the vehicle group for the continuous **(B)** and early **(A)** treatment paradigms. No significance was noted between the two groups for the late treatment study **(C, D).** Data are expressed as mean ±SEM (n = 7-23 animals per treatment group).

II-B. αCT-1 Peptide Maintains RPE Cell Integrity Around CNV Lesions

CNV has at least two components, it involves breakdown of the RPE, followed by angiogenesis of the choroidal vasculature. To test whether CNV size also correlated with RPE cell integrity, a subset of mice (vehicle group and animals treated for 6 days with αCT-1) were sacrificed 7 days after CNV induction and the RPE/choroid was flatmounted. The flatmounts were histologically analyzed for the cell junction markers ZO-1 and occludin. In the vehicle-treated animals, ZO-1 and occludin staining revealed a large halo of unhealthy RPE cells surrounding the CNV lesion **(Fig. 5A, C)**. Unhealthy was defined as cells having lost their junctional markers or having lost their normal hexagonal shape. The diameter of this halo was significantly reduced (P <0.05) by the αCT-1 peptide for both cell junction markers by ~30% **(Fig. 5B, D and Fig. 6)**. This data suggested that the αCT-1 peptide diffuses to the site of the lesion in the RPE/BrM where it is needed to stabilize tight junctions, preventing the breakdown of the RPE layer, thereby limiting the size of the CNV lesions.

Figure 5

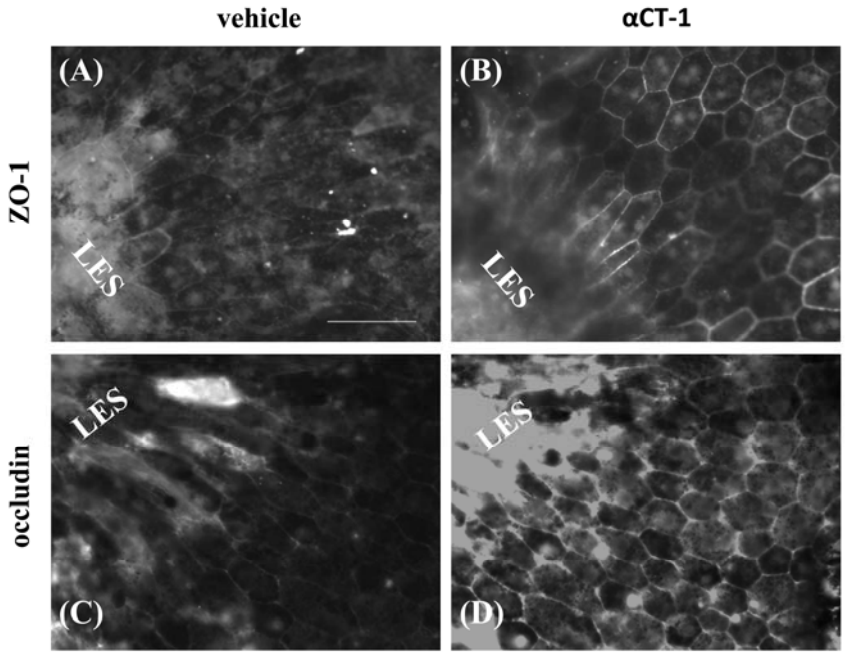

Figure 5. RPE integrity in αCT-1 compared to vehicle-treated mice (qualitative approach). On day 6 after the induction of CNV, eyes were enucleated and RPE/choroid eyecups were stained for two different cell junction markers ZO-1 **(A, B)** and occludin **(C, D**). Representative images for each cell junction marker are presented, depicting the differences in the diameter of unhealthy cells (peri- lesion area) surrounding the lesion (LES) in the control group compared to the αCT-1-treated animals.

Figure 6

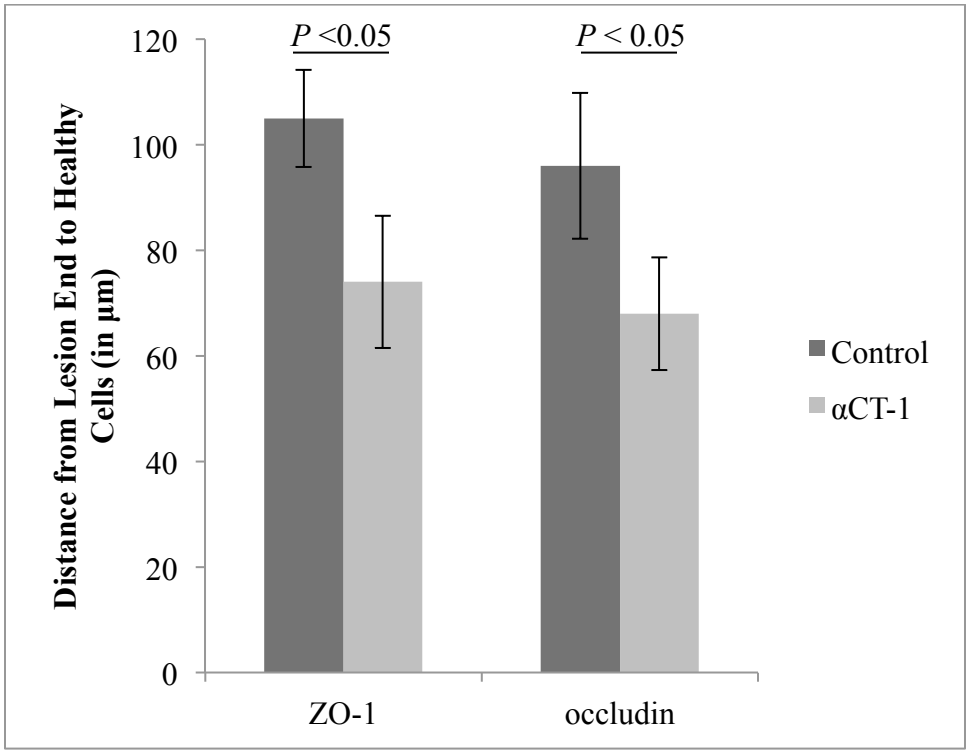

Figure 6. RPE integrity in αCT-1 compared to vehicle-treated mice (quantitative approach). Quantitative comparisons of lesion distances for each cell junction marker and treatment group reveals that αCT-1 significantly (P <0.05) reduced the lesion distance for ZO-1 as well as occludin (in µm; ZO-1: control 105 ±9.2 versus αCT-1 74 ±12.5; occludin: control 96 ±13.8 versus αCT-1 68.3 ±10.7). Data are expressed as mean ±SEM (n = 7-8).

II-C. Effects of the αCT-1 Peptide on Retina Function in CNV

We have shown previously that CNV size correlates with loss of retinal function as measured by Ganzfeld ERGs.[53] Retinal function was assessed by recording dark-adapted ERG amplitudes. These readings allow for the analysis of the light sensitivity of the rod photoreceptors (a-wave) and the sensitivity of the bipolar cells to the cessation of glutamate release from the stimulated photoreceptors (b-wave). Vehicle- and αCT-1-treated animals (n=8 per group) were compared after completing the CNV study with the early continuous treatment regimen **(Fig. 7A, B)**. The data revealed a ~15-20% reduction of ERG responses in control animals when compared to the αCT-1 group. ERG measurements were made for 6 different light intensities (-40, -30, -20, -10, -6 and 0 dB of attenuation). Using a t-test for comparison at individual light intensities, αCT-1-treated animals had significantly higher amplitudes at all intensities for both a- and b-waves, when compared to controls, which was confirmed using a repeated measure ANOVA over the different light intensities for both a-and b-waves ($P < 0.001$).

Figure 7

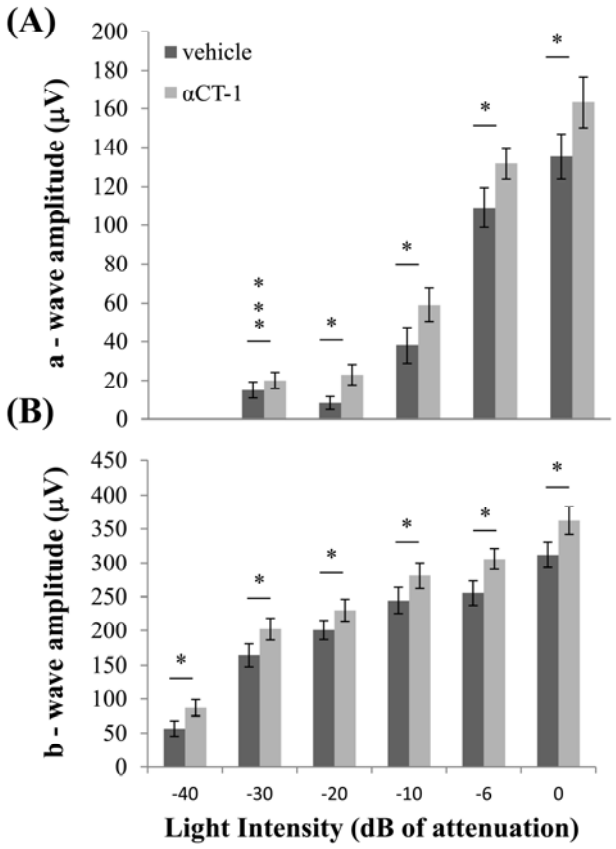

Figure 7. Retina Function of αCT1- versus vehicle-treated animals. Mice were dark-adapted and single-flash recordings were performed with maximum light intensity of 2.48 scotopic cd*s/m^2. (A-B) A- and b-wave amplitudes revealed a significant reduction in amplitude for the brighter light intensities (-40, -20, -10, -6 and 0 dB). Statistical significance (* P <0.05), determined by repeated measure ANOVA, is indicated for the range of light intensities tested in the study. Animals treated with αCT1 peptide lost less visual function than those treated with vehicle over the entire range of light intensities studied. Data are expressed as mean ±SEM (n = 7-8 animals per treatment group).

III. Effects of αCT-1 in a light damage model

III-A. Effects of the αCT-1 Peptide on RPE Cell Integrity in a light damage model

It has been shown that hyper-activation of the retina via bright-light exposure leads to photoreceptor cell death in mice in part due to increased VEGF-mediated RPE permeability.[56] To investigate the effects of the αCT-1 peptide on RPE cell integrity, RPE damage was triggered using a light-damage model (3000 lux of white light for 3 hours) in Balb/c mice. Cell morphology was determined via ZO-1 and occludin immunohistochemistry in RPE flatmounts (**Fig. 8A, B**). Cell profiler software was used to determine the tiling pattern of the RPE and its morphology for animals that were pretreated with the αCT-1 peptide (5 mM) compared to vehicle prior to bright light exposure (**Table 1**). Light damage reduced the number of cells with ZO-1 staining (**Table 1**, ZO-1) by ~30%, as evidenced by the significant drop in cell count (P = 0.004), the number of neighbors (P = 0.008) and the area covered (P = 0.05, when compared to no light damage). In addition, cellular morphology was altered as evidenced by significant changes in form factor (P = 0.017) and eccentricity (P = 0.002). αCT1 treatment significantly preserved RPE morphology and cell counts. Similar results were obtained when analyzing occludin distribution by immunohistochemistry and image analysis (**Table 1**, occludin).

Figure 8

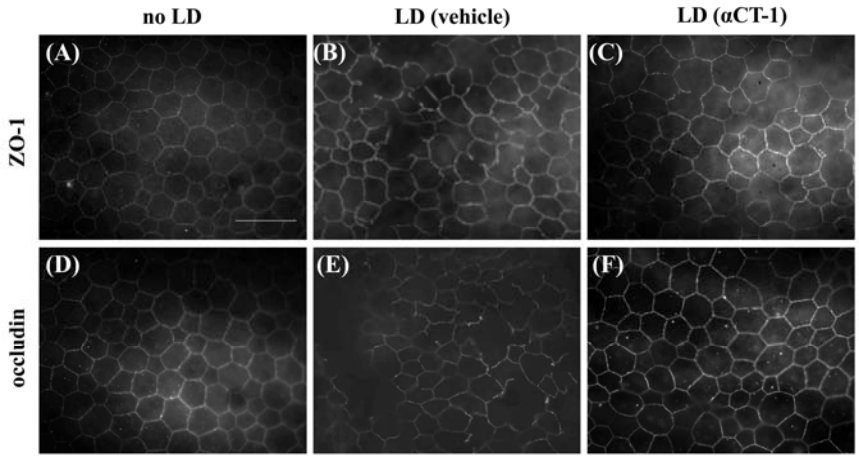

Figure 8. RPE morphology following light-damage. Balb/c mice were exposed to bright light (3000 lux) for 3 hours, and sacrificed and eyes enucleated after 24 hours. RPE morphology was analyzed by immunohistochemistry for ZO-1 **(A-C)** and occludin **(D-F)** on RPE/choroid flatmounts from the respective treatment groups, no light damage controls **(A, D)**, light damage treated with vehicle (B, E) and light damage treated with αCT-1 peptide **(C, F)**.

Table 1

	(mean values):	**no LD**	**LD Vehicle**	**LD αCT1**
ZO1	Cell count	60 ±2	44 ±5*	56 ±3
	Form factor	0.82 ±0.02	0.76 ±0.04*	0.79 ±0.03
	Eccentricity	0.64 ±0.01	0.69 ±0.02*	0.65 ±0.01
	Number of neighbors	5.7 ±0.8	4.3 ±1.3*	5.4 ±1.1
	Perimeter	79 ±4	52 ±8*	71 ±6
	Area covered	96 ±9	62 ±13*	93 ±10
occludin	Cell count	63 ±3	48 ±7*	59 ±2
	Form factor	0.79 ±0.02	0.71 ±0.03*	0.77 ±0.04
	Eccentricity	0.62 ±0.01	0.68 ±0.02*	0.64 ±0.02
	Number of neighbors	5.8 ±0.7	4.1 ±0.9*	5.6 ±0.8
	Perimeter	76 ±6	49 ±12*	69 ±8
	Area covered (%)	95 ±7	64 ±9*	91 ±8

Table 1. Morphometric analysis to quantify changes in retinal pigment epithelium cells in ZO-1- and cccludin-stained images using CellProfiler. Measurements were significant ($P < 0.05$) between the no light damage controls (no LD) and the light-damaged PBS-treated animals (LD vehicle) for all morphometric factors analyzed. No significance in morphometric measurements were identified between light-exposed animals that were treated with αCT-1 (LD αCT-1) and subjects that were never exposed to bright light (no LD, control).

III-B. Establishing a Therapeutic Window for the αCT-1 peptide in the light damage model

Using the same light damage model as in previous experiment (3000 lux for 3 hours), we wanted to investigate the drug's therapeutic window of αCT-1. To evaluate whether loss of barrier function in light damage can be reduced using a delayed treatment paradigm or if pre-treatment with the peptide is necessary to prevent RPE damage, we administered one dose of eye drops (5mM; 10 μL per eye) at either -4, -2, -1, +1, +4 or +6 hours with respect to the time of bright light exposure (**Table 2)**. The RPE was collected 24 hours after light exposure and stained with ZO-1. Animals pre-treated only with one dose of αCT-1 significantly ($P < 0.05$) preserved RPE morphology and cell counts for most morphometric factors, while delayed treatment resulted in no significant differences between treated animals and vehicles. Thus, the breakdown of the RPE can be rescued by supplying an effective dose of αCT-1 prior to injury in a light damage model.

Table 2

(mean values):	**no LD**	**LD vehicle**	**LD αCT-1 (-4 hour)**	**LD αCT-1 (-2 hour)**	**LD αCT-1 (-1 hour)**	**LD αCT-1 (+1 hour)**	**LD αCT-1 (+4 and +6 hours)**
Cell Count	62 ±3	42 ±5	**57 ±2***	54 ±5	50 ±4	52 ±3	46 ±4
Form Factor	0.81 ±0.02	0.75 ±0.02	**0.79 ±0.01***	**0.80 ±0.02***	0.77 ±0.03	0.75 ±0.02	0.76 ±0.03
Eccentricity	0.63 ±0.01	0.71 ±0.01	**0.66 ±0.1***	**0.67 ±0.03***	**0.65 ±0.01***	0.69 ±0.03	0.7 ±0.02
Number of Neighbors	5.8 ±0.7	4.3 ±0.6	5.2 ±1.2	**5.3 ±0.7***	**5.4 ±1.3***	4.7 ±0.8	4.5 ±0.9
Perimeter	76 ±4	53 ±6	**69 ±4***	**72 ±5***	**73 ±5***	65 ±8	51 ±11
Area Covered (%)	97 ±6	64 ±8	**92 ±2***	**88 ±4***	**91 ±3***	73 ±11	60 ±10

Table II. Morphometric analysis to quantify changes in retinal pigment epithelium cells in ZO- 1-stained images using CellProfiler to determine the therapeutic window for αCT-1. Animals were treated at the indicated times (-4, -2, -1, +1, +4 and +6 hours) with zero representing the time of Light ON. Protection was identified (i.e, measurements were significant; $P < 0.05$) for the majority of morphometric factors analyzed for the treatment groups that initiated treatment prior to the onset of light damage.

Specific Aim 1 Conclusions

A novel peptide, αCT-1, was developed and has been identified to have anti-inflammatory and regenerative properties.[45, 50, 51] αCT-1 is a soluble 25 amino acid peptide (3597.33 MW) that has a compact 2-domain design based on linkage of an antennapedia (a cellular membrane transport peptide) internalization domain (1-16 amino acids; RQPKIWFPNRRKPWKK) to the C-terminal PDZ binding domain of Cx43 (17-25 amino acids; RPRPDDLEI). In the current study we were able to show translocation of the αCT-1 peptide to the RPE following corneal application. To determine the therapeutic possibility of targeting Cx43 pathways with αCT-1 in the treatment of AMD, we chose two animal models that mimic VEGF-dependent loss of RPE barrier function: the mouse model of choroidal neovascularization, and the light-induced loss of barrier function in Balb/c mice. In both of those models, anti-VEGF blocking strategies have been shown to prevent or reduce pathology.[56, 61] Here we showed that the αCT-1 peptide significantly reduced the αCT-1 peptide significantly reduced fibrovascular scarring as well as the amount of fluid leakage into the subretinal space when applied immediately after laser photocoagulation. The reduction of CNV development correlated with healthier RPE cells found closer to the lesion site in the αCT-1-treated animals compared to the vehicle group. A reduction in CNV development also correlated with improved retinal function as shown in the higher rod ERG a- and b-wave amplitudes in mice treated with the peptide. Data from the light-damage model indicated that the αCT-1 peptide also improved cell morphology in this model of RPE barrier loss as long as the peptide was applied prior to RPE injury due to light damage. These data show that the αCT-1 peptide preserves RPE barrier function in these models.

Chapter 3: Specific Aim 2

Examine effects of the αCT-1 peptide *in vitro* on ARPE-19 cells to study the drug's mechanism of action

In order to study αCT-1's mechanism of action, we examined its effects on ARPE-19 cells, an established human RPE cell monolayer system. These cells grow in tight polarized monolayers, forming an apical and basal side. Intact tight junctions have been shown to be necessary for efficient removal of fluid from the subretinal space as well as the barrier function of the RPE.[62] This accumulation of subretinal fluid has been reported in AMD, implying impaired barrier function in AMD. Barrier function requires a stable transepithelial resistance (TER), where high TER is indicative of robust RPE barrier properties. Maximal TER values are reached within 2-3 weeks after reaching confluency (40- 45 Ωcm^2).[63] Furthermore, Ablonczy et al showed that adding VEGF to ARPE-19 cells renders a significance decrease in TER, demonstrating increased RPE permeability.[64]

In the RPE, the peptide could act on tight junctions, gap junctions as well as hemichannel activity. Two members of the connexin family are expressed in the RPE: Cx43 as well as Cx46.[28] Cx43 hemichannels play a critical role in providing a paracrine and autocrine route for intercellular communication, releasing extracellular messengers, such as NAD+ and ATP.[40, 41] It has been proposed in heart- and wound injury that the drug is effective via two possible mechanisms.[45] αCT-1 mediates the localization of Cx43 hemichannels to gap junctions, thus, the size of the gap junction plaque increases due the translocation of hemichannels from the perinexus to the site of the gap junction plaque. Thus, one possible mechanism would be that increased stability of gap junctions could allow for a

more coordinated cellular activity, stabilizing the cells. coordinated cellular activity, stabilizing the cells. It is equally plausible that decreasing hemichannel activity results in decreased release of extracellular messengers like ATP, preventing an inflammatory response with VEGF and other cytokines and cell death associated with elevated ATP release.[40, 41, 45] A stabilization of gap junctions can also foster the integrity of tight junctions in RPE cells. ZO-1 binding to tight junction proteins reinforces the anchoring between tight junction proteins and the cytoplasmic actin, reducing fluid accumulation in the subretinal space.[30, 62] Thus, the deterioration of the RPE can be mediated by any one of the three cell junctions breaking down.

In order to study which cell junction is affected by αCT-1, we inhibited gap junction communication as well as hemichannel activity in ARPE-19 cells and analyzed the resulting TER outcome. Gap junctions were blocked utilizing 18-β-glycerrhetinic acid (18-beta-GCA) and hemichannel activity was inhibited by adding apyrase to the cells.[65, 66] Apyrase catalyzes the hydrolysis of ATP, rendering it impossible to bind to purinergic P2 receptors when released via hemichannels.[66, 67] Given that elevated levels of VEGF can be the result of increased hemichannel activity as well as VEGF playing a critical role in AMD development, we wanted to see if αCT-1 would ameliorate its effects in a TER assay. Following the assay, the cells were stained with cell junction markers to investigate their tiling pattern between the respective treatment groups.

Material and Methods

ARPE-19 Cell Cultures

ARPE-19 cells, a human RPE cell line, was expanded in Dulbecco's modified Eagle's medium (DMEM) (Invitrogen) with 10% fetal bovine serum and antibiotics as previously described.[68] These cells generate a polarized RPE cell monolayer when plated on Transwell filters (3450; Costar). Cells were grown on permeable membrane inserts in the presence of DMEM with 10% fetal bovine serum and antibiotics. After cells became confluent, serum was reduced to 2%. Cells were exposed to serum-free media the last two days prior to the measurements. Barrier function requires a stable transepithelial resistance (TER), where high TER is indicative of the robust RPE barrier properties afforded by tight junctions.[64] TER was monitored with an epithelial volt-ohm meter (World Precision Instruments) equipped with an STX2 electrode. Maximal TER values (40-45 Ωcm^2) are reached within 2-3 weeks after cells reach confluency.[64] The TER value for cell monolayers was determined by subtracting the TER for filters without cells, and the percent TER decrease was calculated using the starting value as the reference. Agents used for the TER assays were VEGF165 (SRP4363; Sigma Aldrich), 18-beta glycyrrhetinic acid (G10105, Sigma Aldrich) and apyrase (M0398S; NEB).

Immunofluorescence Staining

Staining was also performed on ARPE-19 cells that were grown on transwell filters (3450; Costar). Cells were either incubated in antibodies recognizing ZO-1 (1:200; Invitrogen), □ccluding (1:200; Invitrogen) or connexin43 (1:300; Sigma Aldrich) in blocking solution (10% normal goat serum, and 0.4% Triton-X in tris-buffered saline).

All before mentioned antibodies are rabbit polyclonal; thus, Alexa Fluor 488 goat-anti-rabbit (1:500; Invitrogen) was used as the secondary antibody. If necessary, cells were flattened using relaxing cuts and cover-slipped using Fluoromount (Southern Biotechnology Associates, Inc., Birmingham, AL). All immunohistochemistry experiments included a no-primary antibody control. Staining of cells was examined via fluorescence microscopy (Zeiss, Thornwood, NY) equipped with a digital black-and-white camera (Spot camera; Diagnostic Instruments, Sterling Heights, MI).

Statistical Analysis

Data are presented as mean ± SEM. Single comparisons were analyzed by *t* test analysis, accepting a significance level of $P < 0.05$.

Results

I. Effects of the αCT-1 Peptide on VEGF-Mediated TER Reduction

For mechanistic studies, we switched to assessing barrier function in ARPE-19 cells, a human RPE cell line. These cells were grown on transwell plates where they establish a polarized monolayer. An indication of proper tight junction integrity is high TER.[64] VEGF has previously been shown to alter tight junctions and promote leakage in RPE cells, resulting in a reduction in TER. This loss in VEGF-induced TER can be prevented by co-administration of a VEGF-R2 receptor antagonist.[64] Here we confirmed that VEGF leads to a reduction in TER in a time-dependent manner (**Fig. 9A**), which can be ameliorated by pre-incubating the cells with αCT-1. **Figure 9B** exhibits a protective effect of the peptide even up to a VEGF concentration of 30 ng/mL, a very high level of insult. A 60ng/mL VEGF concentration leads to a complete loss of barrier function as indicated by a 100% drop of TER (data not shown). Pre-treatment with αCT-1 could not rescue this level of stress to the RPE. 24 hours after treating cells with increasing concentrations of VEGF, the cells were stained with ZO-1 in order to look at their morphology. The decreasing TER results matched the level of disruption in the cell's tiling pattern, the corollary is true, and the protective effect of αCT-1 correlated with a more undisrupted cell shape.

Figure 9

(A)

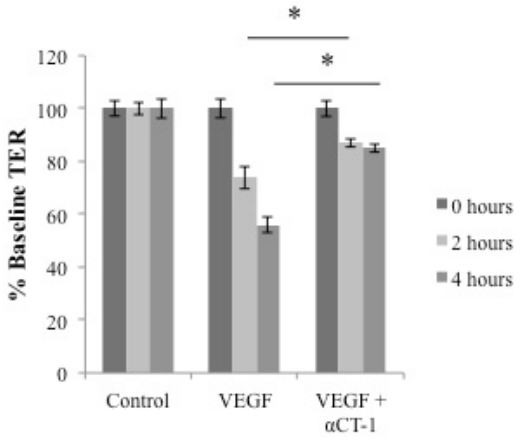

(B)

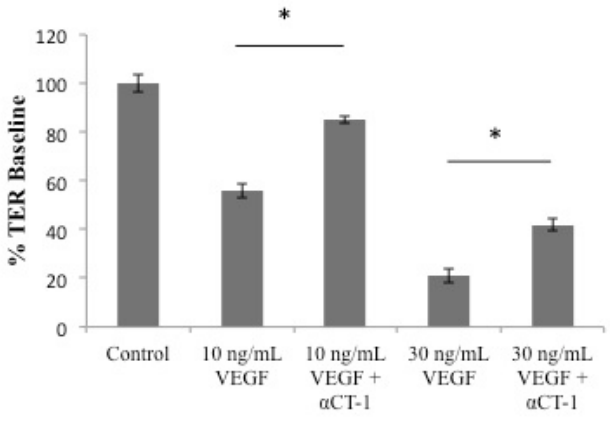

(C)

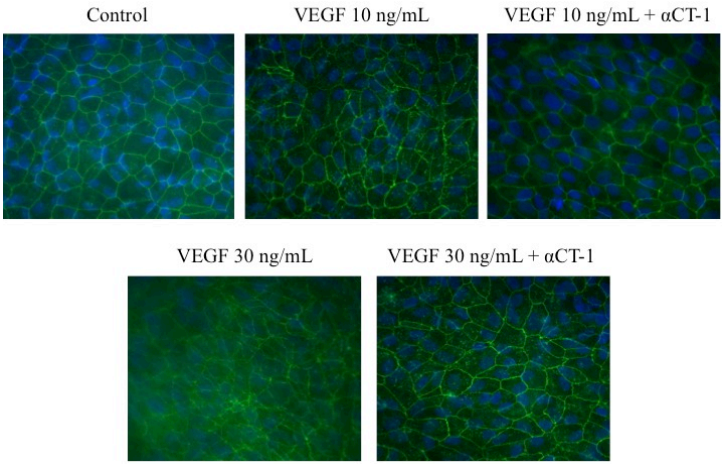

Figure 9. **Effects of apical application of VEGF on TER on ARPE-19 cells grown on transwell plates**. (**A)** TER was measured via a volt-ohm meter with an STX2 electrode. VEGF (10 ng/mL) significantly (# P <0.01) reduced TER by 2 and 4 hours post-application. Pretreatment with 100 μM αCT1 ameliorated the drop in TER at both time points. Data are expressed as mean ±SEM (n = 3 per treatment group). (**B)** Pretreatment with 100 μM αCT1 was even protective against a 3-fold concentration of VEGF (30 ng/mL), however, a VEGF concentration of 60 ng/mL resulted in irreparable damage that

could not be rescued by αCT1. Data are expressed as mean ±SEM (n = 3 per treatment group). (**C**) Representative images of ARPE-19 cells stained with ZO-1 and DAPI for each treatment group referenced in **Figure 9B**.

II. Effects of the αCT-1 Peptide on Gap Junction Function and on ATP Release via Hemichannel Activity

Since there is evidence that VEGF can transiently disrupt endothelial gap junction communication,[37] we tested whether αCT-1 might act by modulating gap junction function by adding the gap junction blocker, 18-β-GCA (0.1 mM), to the ARPE-19 TER assay (**Fig. 10A**).[65] Administration of the gap junction inhibitor alone had little effect on TER. Additionally, there was no significant difference in TER between cells that received VEGF (10 ng/mL) only and wells where VEGF and 18-beta GCA was added together. Interestingly, the addition of αCT-1 peptide ameliorated the effects of VEGF-mediated TER reduction, even in the presence of 18-β-GCA.

Another mechanism of connexin-dependent cell communication involves extra-cellular or paracrine communication via unpaired hemichannels.[66] These channels allow for communication between the intracellular compartment and the extracellular environment. The predominant messenger released by hemichannels is ATP that can act via autocrine signaling on purinergic receptors. Extracellular ATP is important for calcium signaling activation as well as regulating ion and fluid transport in the RPE.[41, 66] Rhett and colleagues showed that αCT1 can recruit hemichannels into gap junctions, thereby indirectly reducing the pool of hemichannels available for signaling.[32] If VEGF-treatment mediates the release of hemichannel ATP release, apyrase (1 U/mL), an ATP/ase and ADP/ase should prevent the VEGF-induced loss in TER.[67] Analysis of TER (**Fig. 10B**) revealed that applying apyrase alone significantly (P <0.05*)* reduced resistance, suggesting that ATP signaling is important for RPE barrier function. However, the TER

decrease elicited by applying apyrase and VEGF together to ARPE-19 cells was not significantly different (P >0.05) from the TER reduction seen by treating with VEGF alone. Application of αCT1 peptide ameliorated the effects of VEGF and apyrase. **Figure 10C** shows the immunohistochemistry images corresponding to the treatment group from the gap junction inhibitor study. ARPE-19 cells were stained with ZO-1 24 hours after the TER assay. Again, αCT1 maintained the regular shape of the cells compared to the ARPE-19 cells that were exposed to VEGF and 18-β-GCA.

Together, these data suggest that the protective effect of αCT1 on VEGF-induced loss in barrier function is not mediated by αCT1's effect on gap-junctions or hemichannels.[31]

Figure 10

(A)

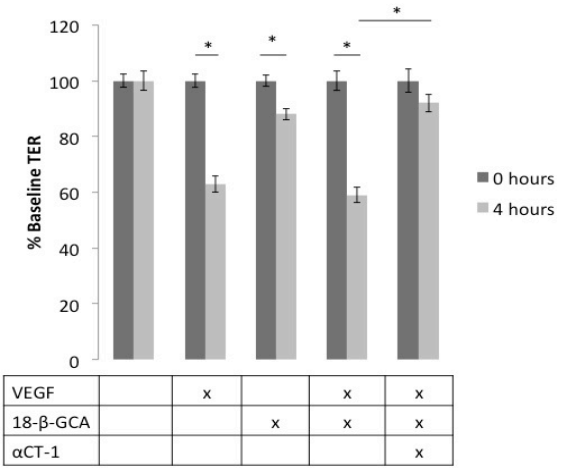

(B)

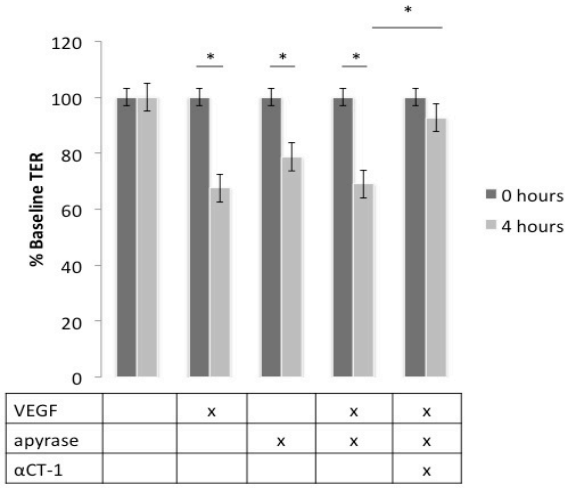

(C)

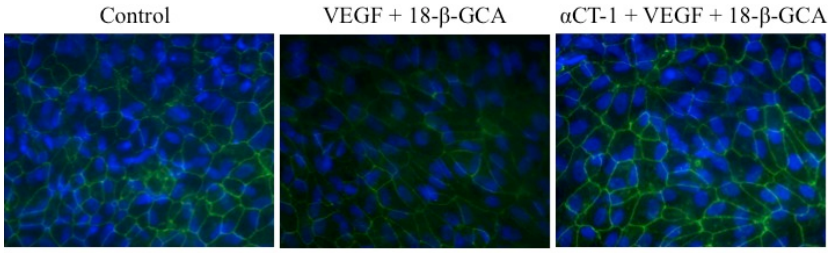

Figure 10. **Determining the contribution of gap junctions and hemichannels on protection by αCT1 on VEGF-mediated loss in barrier function.** (**A**)The TER reduction seen by a sole VEGF (10 ng/mL) administration is not significantly different (P <0.05) from the the TER reduction noted by applying VEGF (10 ng/mL) and 18-β-GCA (0.1 mM). (**B**) Apyrase alone significantly (P <0.05) reduced TER; however, apyrase in addition with VEGF (10 ng/mL) provided no synergistic effect compared to VEGF (10 ng/mL) alone. Data are expressed as mean ±SEM (n = 3 per treatment group). (**C)** Representative images of ZO-1 stained ARPE-19 cells used in the gap junction inhibitor study.

Specific Aim 2 Conclusions

The mechanism of action for αCT-1 is based on the modulation of the interaction between Cx43 and its C-terminal binding partners, including ZO-1. ZO-1 is a critical cell junction protein and it regulates the cellular distribution of Cx43, providing a control point for dynamic switching between gap junction communication and non-junctional hemichannel communication.[32, 33] In order to determine a potential mechanism of action of the compound, we investigated tight junction integrity as well as Cx43-mediated gap and hemichannel communication. TER assays are a simple measure to quantify barrier integrity of RPE cells.[64] TER assays on ARPE-19 cells were conducted to determine which cellular junctions might be affected by VEGF administration and if the αCT-1 peptide would ameliorate those effects. VEGF is known to induce tight junction permeability by trafficking occludin fragments away from the tight junction site as well as by occludin phosphorylation.[16, 35] In addition, VEGF transiently disrupts gap junction communication in endothelial cells.[37] Here we found that 100 μM of αCT-1, a concentration shown to be biologically active in HeLa cells[31] was found to prevent the loss of barrier function in RPE cells induced by 10 ng. ZO-1 stained images of ARPE-19 cells that received an apical application of VEGF verify said disruption of cellular junctions and exhibit longer irregular cell shapes compared to controls. Pre-treatment with αCT-1 maintained a more regular cell shape even with high levels of VEGF, demonstrating its preventive effects on VEGF-induced insults to the RPE.

Blocking gap junction communication in ARPE-19 cells via the gap junction inhibitor, 18-beta-GCA, had little effect on the barrier function in the TER assay, and 18-beta-GCA

did not increase the effect afforded by VEGF alone. However, αCT1 did prevent the loss of TER when VEGF and 18-beta GCA were co-administered. These data suggest that the mechanism of action of αCT-1 did not involve modulating gap junction communication. Another mechanism by which the αCT-1 peptide could stabilize RPE barrier function is via gap junction hemichannel activity. ATP is one of the most abundant extracellular signaling molecules and plays a pivotal role in intercellular communication via autocrine and paracrine signaling, and its release is mediated by hemichannels.[67] ATP has been shown to both increase and decrease endothelial barriers, based on whether the effect is mediated by ATP or its metabolite, adenosine.[69] Furthermore, there is evidence that the release of ATP can promote wound healing in epithelial cells.[70] The latter might be the reason why disrupting ATP communication via the ATP diphosphohydrolase apyrase resulted in a significant decrease in TER when added to the monolayers. If the VEGF effects on TER were to involve ATP-mediated effects, co-administering VEGF and apyrase should have altered the degree of change produced by VEGF alone. However, adding apyrase together with VEGF showed no greater TER reduction than adding VEGF alone. Furthermore, addition of αCT-1 in these assays showed no additional protective effect. Together, these data suggest that αCT-1 may stabilize barrier function by preventing the disassembly of tight junctions by a mechanism independent of gap-junction or hemichannel function.[31]

Chapter 4: Discussion

Overall Conclusion

αCT1 is a peptide-based therapeutic that modulates the activity and signaling pathways mediated by the transmembrane protein, Cx43. Here we analyzed the effects of αCT-1 in *in vivo* and *in vitro* models of VEGF-dependent RPE damage. The main results of the *in vivo* components this study were as follows: (1) αCT-1 delivered topically via eyedrops accumulated in the RPE where it can be detected by immunohistochemistry; (2) αCT-1 significantly reduced laser-induced CNV when applied during the initiation or trigger phase of CNV development rather than during the growth phase; and (3) αCT-1 also significantly improved RPE morphology after bright-light exposure, a stimulus that alters RPE morphology in a VEGF-dependent manner. The *in vitro* RPE assays suggested a mechanism of action that was separate from gap- or hemichannel-mediated cell-cell communication and involved αCT-1 prevention of VEGF-induced loss of transepithelial resistance via the stabilization of tight junctions. Taken together, the data suggested that the stabilization of tight junctions via targeting Cx43 signaling using αCT-1 may serve as a new treatment paradigm for both wet and dry AMD.

Discussion

The RPE is a barrier epithelium located between the retina and the choroid. The outer blood retina barrier is essential to proper functioning of the eye as the epithelial barrier supports nutrient and solute transport while preventing infiltration of cells (choroidal epithelial cells or inflammatory cells) into the subretinal space.[8] Together with its basement membrane, BrM, and the RPE plasma membranes, the primary cellular

determinant of the RPE barrier function is made up by the tight junctions between the RPE cells in the monolayer making up the primary cellular determinant of the RPE barrier function. RPE damage and blood retina barrier loss is a common feature in dry and wet AMD, as well as diabetic retinopathy, and the formation of macular edema. Blood retina barrier loss involves inflammation, angiogenesis, and oxidative stress. VEGF and other growth factors are involved in mediating loss of barrier function in the RPE as well as angiogenesis and choroidal neovascularization. However, the role that VEGF plays in dry AMD is yet to be determined. It is known that elevated levels of VEGF alone is not sufficient to cause any type of AMD, rather an injury to the RPE has to occur that causes an imbalance in VEGF secretion by the RPE.[8, 71] Given that VEGF receptors are located on the apical side, the elevated secretion of VEGF towards the apical side causes a disassembly of tight junctions due to the disruption of ZO-1 organization, generating further RPE permeability.[30]

Our data show that the αCT-1 peptide prevents VEGF-mediated breakdown of the barrier function and stabilizes RPE tight junctions. In aortic endothelial cells, Src, ERK, JNK and PI-3 kinase/Akt, signaling leads to serine/threonine phosphorylation and the redistribution of ZO-1 and occludin.[48] The effects on tight junction stability may occur indirectly, by the well characterized anti-inflammatory effect of αCT1 (inflammation causes tight junction disassembly),[49-51] or by promoting the extent of intercellular adhesion mediated by gap junctions, independent of their intercellular channel function, as we have reported previously.[11, 12] αCT-1 may also have direct effects on tight junction stability. The C-terminus of Cx43 and related connexins are the only PDZ-binding

ligands known to interact with the ZO-1 PDZ2 domain. For example, a phage display-based search for PDZ2 ligands was unable to identify further binding peptides.[52] However, the PDZ2 domain does mediate homomeric interactions with other PDZ2 domains, enabling the formation of domain-swapped ZO-1 homodimers.[53] ZO-1 dimerization is essential for claudin polymerization, and tight junction formation and stability in vivo.[53-55] Domain-swapped PDZ2 dimerization is also necessary for high affinity binding of the Cx43 C- terminus to ZO-1.[56] Endogenous Cx43 C-termini are not thought to interact directly with the macromolecular complexes forming tight junctions. However, the presence of free Cx43 C- termini in the form αCT-1 could provide for ligand-based stabilization of ZO-1 homodimers – via αCT-1 binding to the high-affinity binding pocket generated by PDZ2-PDZ2 interaction. αCT-1 may thus stabilize tight junctions and increase barrier function by directly interacting with dimerized PDZ2 domains, enhancing the stability of the ZO-1-containing quaternary complexes necessary for tight junction formation and maintenance. Ongoing studies are being performed to determine whether enhancement of PDZ2-PDZ2 interaction may be the molecular mechanism by which αCT-1 protects and prevents dedifferentiation of RPE.

An additional potential mechanism that deserves investigation is based on observations that at the tissue level, αCT-1 treatment is associated with reduction in pro-inflammatory cytokines and decreased inflammatory responses.[57-59] In AMD, this mechanism of action may mediate responses elicited from RPE cells, or inflammatory cells such as Mueller cells, astrocytes and glial cells as well as invading leukocytes, all of which express Cx43. Inflammation has been shown to contribute to CNV lesion size and fluid leakage in AMD

as well as mouse models.[60] Likewise, a chemokine-mediated inflammatory response has been shown after light-damage, involving RPE, Mueller cells and activated microglia[61]. In addition, in the rat it has been reported that Cx43 expression in the choroid co-localizes with markers of oxidative stress and inflammation.[62] These additional mechanisms will be investigated in future studies.

The most widely used treatment for wet AMD is intraocular anti-VEGF injections, whereas no treatment is available for dry AMD. Given that the αCT-1 peptide reduced AMD-like pathology in two in vivo mouse models via eye drop administration, targeting connexin signaling may serve as a promising new treatment paradigm for both wet and dry AMD, as well as other retinal diseases in which the RPE barrier is affected.

References

1. Kozlowski MR. RPE cell senescence: a key contributor to age-related macular degeneration. *Medical hypotheses* 2012;78:505-510.
2. Brown; MM, Brown; GC, Stein; JD, Roth; Z, Campanella; J, Beauchamp GR. Age-related macular degeneration: economic burden and value-based medicine analysis. *Canadian Journal of Opthalmology* 2005;40:277-287.
3. Group TEDPR. Prevalence of Age-Related Macular Degeneration in the United States. *Arch Ophthalmol* 2004;122:564-572.
4. Whitcup SM, Sodhi A, Atkinson JP, et al. The role of the immune response in age-related macular degeneration. *Int J Inflam* 2013;2013:348092.
5. Hageman GS, Anderson DH, Johnson LV, et al. A common haplotype in the complement regulatory gene factor H (HF1/CFH) predisposes individuals to age-related macular degeneration. *Proceedings of the National Academy of Sciences of the United States of America* 2005;102:7227-7232.
6. Gold B, Merriam JE, Zernant J, et al. Variation in factor B (BF) and complement component 2 (C2) genes is associated with age-related macular degeneration. *Nature genetics* 2006;38:458-462.
7. Ambati J, Fowler BJ. Mechanisms of age-related macular degeneration. *Neuron* 2012;75:26-39.
8. Strauss O. The Retinal Pigment Epithelium in Visual Function. *Physiological Reviews* 2005;85:845-881.
9. Sun M, Finnemann SC, Febbraio M, et al. Light-induced oxidation of photoreceptor outer segment phospholipids generates ligands for CD36-mediated phagocytosis by retinal pigment epithelium: a potential mechanism for modulating outer segment phagocytosis under oxidant stress conditions. *The Journal of biological chemistry* 2006;281:4222-4230.
10. Zeiss CJ. Animals as models of age-related macular degeneration: an imperfect measure of the truth. *Veterinary pathology* 2010;47:396-413.
11. Wolf G. Lipofuscin and Macular Degeneration. *Nutrition Reviews* 2003;61:342–346.
12. Gregory S. Hagemana, Phil J. Luthertb, Chonga NHV, Lincoln V. Johnsonc, Don H. Andersonc, Mullinsa RF. An Integrated Hypothesis That Considers Drusen as Biomarkers of Immune-Mediated Processes at the RPE-Bruch's Membrane Interface in Aging and Age-Related Macular Degeneration. *Progress in Retinal and Eye Research* 2001;20:705-732.
13. Esen K. Akpek M, Roderick A. Smith M. Overview of Age-related Ocular conditions. *The American Journal Of Managed Care* 2013;19:67 - 75.
14. Kay P, Yang YC, Paraoan L. Directional protein secretion by the retinal pigment epithelium: roles in retinal health and the development of age-related macular degeneration. *Journal of cellular and molecular medicine* 2013;17:833-843.
15. Kannan R, Zhang N, G.Sreekumar P, et al. Stimulation of apical and basolateral vascular endothelial growth factor-A and vascular endothelial growth factor-C secretion by oxidative stress in polarized retinal pigment epithelial cells. *Molecular Vision* 2006;12:649-659.

16. Rao R. Occludin phosphorylation in regulation of epithelial tight junctions. *Ann N Y Acad Sci* 2009;1165:62-68.
17. Peng S, Gan G, Rao VS, Adelman RA, Rizzolo LJ. Effects of proinflammatory cytokines on the claudin-19 rich tight junctions of human retinal pigment epithelium. *Invest Ophthalmol Vis Sci* 2012;53:5016-5028.
18. Fanning AS, Anderson JM. Zonula occludens-1 and -2 are cytosolic scaffolds that regulate the assembly of cellular junctions. *Ann N Y Acad Sci* 2009;1165:113-120.
19. Giepmans B. Gap junctions and connexin-interacting proteins. *Cardiovascular Research* 2004;62:233-245.
20. Rodgers LS, Beam MT, Anderson JM, Fanning AS. Epithelial barrier assembly requires coordinated activity of multiple domains of the tight junction protein ZO-1. *J Cell Sci* 2013;126:1565-1575.
21. L. Gonzalez-Mariscal, A. Betanzos, P. Nava, Jaramillo BE. Tight junction proteins. *Prog Biophys Mol Biol* 2003;81:1-44.
22. Matter K, Balda MS. Signalling to and from tight junctions. *Nature reviews Molecular cell biology* 2003;4:225-236.
23. Umeda K, Ikenouchi J, Katahira-Tayama S, et al. ZO-1 and ZO-2 independently determine where claudins are polymerized in tight-junction strand formation. *Cell* 2006;126:741-754.
24. Shen L, Weber CR, Raleigh DR, Yu D, Turner JR. Tight junction pore and leak pathways: a dynamic duo. *Annual review of physiology* 2011;73:283-309.
25. Meng W, Takeichi M. Adherens junction: molecular architecture and regulation. *Cold Spring Harbor perspectives in biology* 2009;1:a002899.
26. Vladimir A Krutovskikh, Piccoli C, Yamasaki H. Gap junction intercellular communication propagates cell death in cancerous cells. *Oncogene* 2002;21:1989-1999.
27. Sohl G, Willecke K. Gap junctions and the connexin protein family. *Cardiovasc Res* 2004;62:228-232.
28. Quan V. Hoang, Haohua Qian, Ripps H. Functional analysis of hemichannels and gap-junctional channels formed by connexins 43 and 46. *Molecular Vision* 2010;16:1343-1352.
29. Evans WH, Martin PE. Gap junctions: structure and function (Review). *Molecular membrane biology* 2002;19:121-136.
30. Bauer H, Zweimueller-Mayer J, Steinbacher P, Lametschwandtner A, Bauer HC. The Dual Role of Zonula Occludens (ZO) Proteins. *Journal of Biomedicine and Biotechnology* 2010;2010:1-12.
31. Hunter AW, Barker RJ, Zhu C, Gourdie RG. Zonula occludens-1 alters connexin43 gap junction size and organization by influencing channel accretion. *Mol Biol Cell* 2005;16:5686-5698.
32. Rhett JM, Jourdan J, Gourdie RG. Connexin 43 connexon to gap junction transition is regulated by zonula occludens-1. *Mol Biol Cell* 2011;22:1516-1528.
33. Martin P, Parkhurst SM. Parallels between tissue repair and embryo morphogenesis. *Development* 2004;131:3021-3034.

34. Van Itallie CM, Fanning AS, Bridges A, Anderson JM. ZO-1 Stabilizes the Tight Junction Solute Barrier through Coupling to the Perijunctional Cytoskeleton. *Molecular Biology of the Cell* 2009;20:3930-3940.
35. Murakami T, Felinski EA, Antonetti DA. Occludin phosphorylation and ubiquitination regulate tight junction trafficking and vascular endothelial growth factor-induced permeability. *The Journal of biological chemistry* 2009;284:21036-21046.
36. Dorfel MJ, Huber O. Modulation of tight junction structure and function by kinases and phosphatases targeting occludin. *Journal of biomedicine & biotechnology* 2012;2012:807356.
37. Suarez S, Ballmer-Hofer K. VEGF transiently disrupts gap junctional communication in endothelial cells. *Journal of Cell Science* 2001;114:1229-1235.
38. Zhu C, Barker RJ, Hunter AW, Zhang Y, Jourdan J, Gourdie RG. Quantitative analysis of ZO-1 colocalization with Cx43 gap junction plaques in cultures of rat neonatal cardiomyocytes. *Microscopy and microanalysis : the official journal of Microscopy Society of America, Microbeam Analysis Society, Microscopical Society of Canada* 2005;11:244-248.
39. Hunter AW, Jourdan J, Gourdi RG. Fusion of GFP to the Carboxyl Terminus of Connexin43 Increases Gap Junction Size in HeLa Cells. *Cell Communication and Adhesion* 2003;10:211-214.
40. Faigle M, Seessle J, Zug S, El Kasmi KC, Eltzschig HK. ATP release from vascular endothelia occurs across Cx43 hemichannels and is attenuated during hypoxia. *PloS one* 2008;3:e2801.
41. Ward M. Peterson, Chris Meggyesy, Kefu Yu, Miller SS. Extracellular ATP Activates Calcium Signaling, Ion, and Fluid Transport in Retinal Pigment Epithelium. *The Journal of Neuroscience* 1997;17:2324-2337.
42. Palatinus JA, Rhett JM, Gourdie RG. The connexin43 carboxyl terminus and cardiac gap junction organization. *Biochimica et biophysica acta* 2012;1818:1831-1843.
43. O'Quinn MP, Palatinus JA, Harris BS, Hewett KW, Gourdie RG. A Peptide Mimetic of the Connexin43 Carboxyl Terminus Reduces Gap Junction Remodeling and Induced Arrhythmia Following Ventricular Injury. *Circulation Research* 2011;108:704-715.
44. Palatinus JA, Rhett JM, Gourdie RG. Enhanced PKC epsilon mediated phosphorylation of connexin43 at serine 368 by a carboxyl-terminal mimetic peptide is dependent on injury. *Channels* 2011;5:236-240.
45. Ongstad EL, O'Quinn MP, Ghatnekar GS, Yost MJ, Gourdie RG. A Connexin43 Mimetic Peptide Promotes Regenerative Healing and Improves Mechanical Properties in Skin and Heart. *Advances in wound care* 2013;2:55-62.
46. Ghatnekar GS, O'Quinn MP, Jourdan LJ, Gurjarpadhye AA, Draughn RL, Gourdie RG. Connexin43 carboxyl-terminal peptides reduce scar progenitor and promote regenerative healing following skin wounding. *Regenerative medicine* 2009;4:205-223.
47. Rhett JM, Ghatnekar GS, Palatinus JA, O'Quinn M, Yost MJ, Gourdie RG. Novel therapies for scar reduction and regenerative healing of skin wounds. *Trends in biotechnology* 2008;26:173-180.

48. Soder BL, Propst JT, Brooks TM, et al. The connexin43 carboxyl-terminal peptide ACT1 modulates the biological response to silicone implants. *Plastic and reconstructive surgery* 2009;123:1440-1451.
49. Grek CL, Prasad GM, Viswanathan V, Armstrong DG, Gourdie RG, Ghatnekar GS. Topical administration of a connexin43-based peptide augments healing of chronic neuropathic diabetic foot ulcers: A multicenter, randomized trial. *Wound repair and regeneration : official publication of the Wound Healing Society [and] the European Tissue Repair Society* 2015;23:203-212.
50. Ghatnekar GS, Grek CL, Armstrong DG, Desai SC, Gourdie RG. The effect of a connexin43-based Peptide on the healing of chronic venous leg ulcers: a multicenter, randomized trial. *The Journal of investigative dermatology* 2015;135:289-298.
51. Moore K, Bryant ZJ, Ghatnekar G, Singh UP, Gourdie RG, Potts JD. A synthetic connexin 43 mimetic peptide augments corneal wound healing. *Exp Eye Res* 2013;115:178-188.
52. Wong WL, Su X, Li X, et al. Global prevalence of age-related macular degeneration and disease burden projection for 2020 and 2040: a systematic review and meta-analysis. *The Lancet Global Health* 2014;2:e106-e116.
53. Rohrer B, Long Q, Coughlin B, et al. A Targeted Inhibitor of the Alternative Complement Pathway Reduces Angiogenesis in a Mouse Model of Age-Related Macular Degeneration. *Investigative Ophthalmology & Visual Science* 2009;50:3056-3064.
54. Nozaki M, Raisler BJ, Sakurai E, et al. Drusen complement components C3a and C5a promote choroidal neovascularization. *Proceedings of the National Academy of Sciences of the United States of America* 2006;103:2328-2333.
55. Nalini S. Bora, Sankaranarayanan Kaliappan, Purushottam Jha, et al. Complement Activation via Alternative Pathway Is Critical in the Development of Laser-Induced Choroidal Neovascularization: Role of Factor B and Factor H. *J Immunol 2006* 2006;177:1872-1878.
56. Cachafeiro M, Bemelmans AP, Samardzija M, et al. Hyperactivation of retina by light in mice leads to photoreceptor cell death mediated by VEGF and retinal pigment epithelium permeability. *Cell death & disease* 2013;4:e781.
57. Giani A, Thanos A, Roh MI, et al. In Vivo Evaluation of Laser-Induced Choroidal Neovascularization Using Spectral-Domain Optical Coherence Tomography. *Investigative Ophthalmology & Visual Science* 2011;52:3880-3887.
58. Jeffrey Gresh, Patrice W. Goletz, Rosalie K. Crouch, Rohrer B. Structure–function analysis of rods and cones in juvenile, adult, and aged C57BL06 and Balb0c mice. 2003;20.
59. Adam Richards, Alfred A. Emondi J, Rohrer B. Long-term ERG analysis in the partially light-damaged mouse retina reveals regressive and compensatory changes. *Visual Neuroscience* 2006;23:91-97.
60. Narimatsu T, Ozawa Y, Miyake S, et al. Disruption of Cell-Cell Junctions and Induction of Pathological Cytokines in the Retinal Pigment Epithelium of Light-Exposed Mice. *Investigative Ophthalmology & Visual Science* 2013;54:4555-4562.
61. Campa C, Kasman I, Ye W, Lee WP, Fuh G, Ferrara N. Effects of an anti-VEGF-A monoclonal antibody on laser-induced choroidal neovascularization in mice:

optimizing methods to quantify vascular changes. *Invest Ophthalmol Vis Sci* 2008;49:1178-1183.
62. Hartnett ME, Elsner AE. Characteristics of Exudative Age-related Macular Degeneration Determined In Vivo with Confocal and Indirect Infrared Imaging. *Ophthalmology* 1996;103:58-71.
63. K. C. Dunna, A. E. Aotaki-Keenaa, F. R. Putkeyb, Hjelmeland LM. ARPE-19, A Human Retinal Pigment Epithelial Cell Line with Differentiated Properties. *Experimental Eye Research* 1996;62:155-169.
64. Ablonczy Z, Crosson CE. VEGF modulation of retinal pigment epithelium resistance. *Exp Eye Res* 2007;85:762-771.
65. Hutnik CM, Pocrnich CE, Liu H, Laird DW, Shao Q. The protective effect of functional connexin43 channels on a human epithelial cell line exposed to oxidative stress. *Invest Ophthalmol Vis Sci* 2008;49:800-806.
66. Mitchell CH. Release of ATP by a human retinal pigment epithelial cell line: potential for autocrine stimulation through subretinal space. *Journal of Physiology* 2001;534:193-202.
67. Reigada D, Lu W, Mitchell CH. Glutamate acts at NMDA receptors on fresh bovine and on cultured human retinal pigment epithelial cells to trigger release of ATP. *The Journal of physiology* 2006;575:707-720.
68. Thurman JM, Renner B, Kunchithapautham K, et al. Oxidative Stress Renders Retinal Pigment Epithelial Cells Susceptible to Complement-mediated Injury. *Journal of Biological Chemistry* 2009;284:16939-16947.
69. Gunduz D, Aslam M, Krieger U, et al. Opposing effects of ATP and adenosine on barrier function of rat coronary microvasculature. *Journal of molecular and cellular cardiology* 2012;52:962-970.
70. Block ER, Klarlund JK. Wounding sheets of epithelial cells activates the epidermal growth factor receptor through distinct short- and long-range mechanisms. *Mol Biol Cell* 2008;19:4909-4917.
71. Oshima Y, Oshima S, Nambu H, et al. Increased expression of VEGF in retinal pigmented epithelial cells is not sufficient to cause choroidal neovascularization. *Journal of cellular physiology* 2004;201:393-400.